EBV attachment stimulates FHOS/FHOD1 redistribution and co-aggregation with CD21: formin interactions with the cytoplasmic domain of human CD21

Michael B. Gill[1,2,5,*], Jennifer Roecklein-Canfield[1,*], David R. Sage[1,2], Maria Zambela-Soediono[1], Nina Longtine[4,5], Marc Uknis[3] and Joyce D. Fingeroth[1,2,5,‡]

[1]Divisions of Infectious Diseases, [2]Experimental Medicine and [3]Surgery, Beth Israel Deaconess Medical Center and [4]Department of Pathology, Brigham and Women's Hospital and [5]Harvard Medical School, Boston, MA 02115, USA

*These authors contributed equally to this work

‡Author for correspondence (e-mail: jfingero@bidmc.harvard.edu)

Accepted 20 January 2004
Journal of Cell Science 117, 2709-2720 Published by The Company of Biologists 2004
doi:10.1242/jcs.01113

Summary

CD21 is a multifunctional receptor for Epstein-Barr virus (EBV), for C3dg and for CD23. Upon engagement of immune complexes CD21 modulates immunoreceptor signaling, linking innate and adaptive immune responses. The mechanisms enabling CD21 to independently relay information between the exterior and interior of the cell, however, remain unresolved. We show that formin homologue overexpressed in spleen (FHOS/FHOD1) binds the cytoplasmic domain of human CD21 through its C terminus. When expressed in cells, EGFP-FHOS localizes to the cytoplasm and accumulates with actin in membrane protrusions. Plasma membrane aggregation, redistribution and co-localization of both proteins are stimulated when EBV (ligand) binds CD21. Though widely expressed, FHOS RNA is most abundant in the littoral cell, a major constituent of the red pulp of human spleen believed to function in antigen filtration. Formins are molecular scaffolds that nucleate actin by a pathway distinct from Arp2/3 complex, linking signal transduction to actin reorganization and gene transcription. Thus, ligand stimulation of FHOS-CD21 interaction may transmit signals through promotion of cytoskeletal rearrangement. Moreover, formin recruitment to sites of actin assembly initiated by immunoreceptors could be a general mechanism whereby co-receptors such as CD21 modulate intracellular signaling.

Supplemental data available online

Key words: Formin, CD21, Splenic littoral cell, Epstein-Barr virus, Actin cytoskeleton

Introduction

Human CD21 is a multifunctional cell surface glycoprotein that is highly expressed on B-lymphocytes and follicular dendritic cells (FDCs), although it can be detected on many additional cell types. CD21 is the receptor for the C3dg fragment of complement (Iida et al., 1983), for CD23 (Aubry et al., 1994) and human CD21 and is also the major cellular attachment protein for Epstein-Barr virus (EBV) (Fingeroth et al., 1984). CD21 is composed of an extracellular domain consisting of 15-16 short consensus repeat modules, a hydrophobic transmembrane, and a 34 amino acid cytoplasmic domain (Fearon and Carroll, 2000; Moore et al., 1987). The three known ligands all bind within the two N-terminal repeats (Aubry et al., 1994; Fearon and Carroll, 2000), which form a highly flexible domain as demonstrated by crystal structure analysis (Prota et al., 2002).

At present, the role of human CD21 is best understood in the context of the immune response. Many relevant studies have been conducted in mice (Fearon and Carroll, 2000; Holers, 2000), where a related though clearly diverged protein (mCD21/CD35) serves the dual function of both a C3b receptor (complement receptor type 1(CR1)/CD35) and a C3d receptor (CR2/CD21), depending on the pattern of N-terminal splicing. In man, two independent proteins, CD21 and CD35 are synthesized; however, the intracellular domain of human CD21 is most similar to that of mCD21/CD35 (Fingeroth, 1990).

CD21 participates in regulation of antibody (Ab) production through immune complex (C3d-Ab-Ag)-mediated modulation of B-cell receptor (BCR) signaling and internalization, Fc receptor signaling and through retention of pathogenic antigens (including HIV) on FDCs for stimulation of B-cell memory (Cherukuri et al., 2001; Fearon and Carroll, 2000; Moir et al., 2000; Poe et al., 2001; Prodinger, 1999). Interaction of CD21 with CD23 on B-cells is believed to additionally protect B-cells from apoptosis (Bonnefoy et al., 1993). However, the function of CD21 on most other cell types remains unknown.

The attachment of C3d-coated antigen to B-cells and FDCs physically links CD21 to the BCR. Precisely how these interactions culminate in quantitative and qualitative alterations in antibody production is not fully understood. On the resting B-lymphocyte, noncovalent associations between

the extracellular domain of CD21 and other B-cell surface proteins, in particular CD19, that independently mediate B-cell signal transduction have been shown to play a key role (Fearon and Carroll, 2000; Poe et al., 2001). Both mCD21/CD35 and CD19 can co-localize with a retained BCR in cholesterol-rich microdomains (lipid rafts). This event extends the duration and efficiency of intracellular signaling (Cherukuri et al., 2001), augments B-cell proliferation and may logarithmically increase antibody production (Fearon and Carroll, 2000). There is still considerable debate about whether human CD21 regulates ligand (C3d, EBV, CD23) internalization and/or contributes to transmission of any stimuli across the plasma membrane directly and independently of CD19 (Bradbury et al., 1992; Carel et al., 1990; Martin et al., 1994; Tanner et al., 1987).

No direct role for the short conserved cytoplasmic domain of human CD21 in relation to CD21 biology has been established. Recently, human CD46, a related complement receptor, pathogen receptor and a TCR co-receptor, was shown to signal in vivo through its short cytoplasmic domains (cyt1 and cyt2) (reviewed by Lee et al., 2002). Phosphorylation of cyt2 was required to effectively anchor gonococcal pili to the surface of epithelial cells. Furthermore, direct CD46 stimulation of primary T-cells activated Vav while costimulation with CD3 enhanced Rac activation and induced actin reorganization and morphological change (Zaffran et al., 2001). Crosslinking of human CD21 on normal B-lymphocytes by virus and by monoclonal antibodies (mAbs) has also been observed to result in rapid F actin assembly (Melamed et al., 1994) however, the relative roles of CD19 and associated B-cell proteins was not defined.

To investigate the function of the intracellular domain of human CD21, we utilized a yeast two-hybrid assay to identify proteins that directly interact with this region. We show that a member of the formin family, FHOS (formin homologue overexpressed in spleen) (Westendorf et al., 1999) also known as FHOD1 (Koka et al., 2003) interacts with CD21 in mammalian cells through its C terminus.

Formins are multidomain proteins conserved during eukaryotic evolution that directly nucleate actin by a mechanism independent of Arp2/3 complex (Evangelista et al., 2002; Kovar et al., 2003; Li and Higgs, 2003; Sagot et al., 2002b). They serve as molecular scaffolds, recruiting proteins that link cellular signal transduction pathways (Rho family GTPases and src family tyrosine kinases) to actin-binding proteins (profilins) and promote cytoskeletal reorganization (Tanaka, 2000; Zeller et al., 1999) and downstream gene transcription (Copeland and Treisman, 2002; Zeller et al., 1999). Formins are critical for cytokinesis, for the establishment of cell polarity and for control of morphogenesis. FHOS, a human formin first identified in a spleen library has been shown to interact with the small GTPase Rac1, to bind the actin binding protein profilin IIa and to activate the serum response transcription factor in vitro (Tojo et al., 2003; Westendorf, 2001). Recent studies indicate that FHOS can interact with actin monomers and may play a role in the regulation of cell motility and vesicle recycling as well (Koka et al., 2003; Tojo et al., 2003).

By means of fluorescence microscopy we document that engagement of CD21 by extracellular ligand produces coordinate re-localization and clustering of FHOS and CD21 in epithelial cells lacking CD19. This receptor aggregation is greatly diminished in the absence of the C-terminal amino acids of FHOS. We propose a mechanism to explain the interaction of these proteins in vivo, and suggest that anchorage and aggregation of cell surface proteins are an effector function of certain formins. Unexpectedly, FHOS was abundant in the splenic littoral cell, a major constituent of the red pulp of human spleen that lines the splenic sinuses. Littoral cells are believed to play a key role in antigen filtration, though at present little is known about their biology.

Materials and Methods

Construct design

Expression vectors: yeast

cDNA encoding the cytoplasmic 34 amino acids (aa) of CD21 (GenBank accession no. P20023) was amplified using Taq polymerase, Advantage Taq-2 (Clontech) with the forward and reverse primers [5′ GCG*GAATTC*TCAAAACACAGAGAACGCAAT 3′ (*Eco*RI) and 5′ GCG*CTGCAG*GCTGGCTGGGTTGTATGG 3′ (*PstI*)]. cDNA encoding the cytoplasmic 43 aa of CD21 (last 34 + 9 aa of proximal transmembrane domain) was amplified by PCR using the same reverse primer and the forward primer 5′ GCG*GAATTC*TTGATTGTCATTACCTTA 3′ (*Eco*RI). Both PCR products were cloned into the pGBT.C vector (Clontech), placing the insert CD21 sequence in frame with a Gal4 binding domain. The resulting target plasmids were verified by sequencing and named pGBT.C-CD21-CT and pGBT.C-CD21-TMCT respectively.

Bacterial

To generate a glutathione S-transferase (GST)-FHOS CT fusion protein, a 600 bp C-terminal fragment, including nucleotides that encoded the last 199 aa and the stop codon of HeLa FHOS was amplified by PCR using the gene-specific primers: 5′-GCG-*CTCGAG*CAGGCGGCCCGT-3′ (*Xho*I) and 5′-GCG*CTCGAG*T-CACACCTCCAGGC-3′ (*Xho*I). The PCR product was cloned in-frame into the expression plasmid, pGEX4T-1 (Pharmacia), and sequenced (both strands), generating pGEX4T-1-FHOS-CT.

Mammalian

To synthesize pEGFP-FHOS (full length, 1-1164) and pEGFP-FHOSΔCT (C terminus deletion, 1-965), FHOS cDNA was amplified by PCR and cloned into pEGFPC2 (Clontech) using unique restriction sites as follows: FHOS full length primers [MG182 5′ GGG*GTACCG*CATGGCGGGCGGGGAAGACC 3′ (*Kpn*I) and MG113 5′ CG*GGATCC*TCACACCTCCAGGCCAGGACC 3′ (*Bam*HI)] and FHOSΔCT primers [MG 182 and MG196 5′ CGC*GGATCC*TCACGGGGTG TAGCCCAGG 3′ (*Bam*HI)]. To generate pBABE-CD21, CD21 cDNA was cloned into the multiple cloning site of pBABE (Morgenstern and Land, 1990), an eukaryotic expression vector.

Cells

Lines

Raji, Burkitt's lymphoma; Nalm6, B-cell leukemia (a gift from Arnold Freedman, Dana-Farber Cancer Institute); 293T, embryonic kidney line transformed with adenovirus fragments and bearing SV40-T antigen [a gift from Hava Avraham, Beth Israel Deaconess Medical Center (BIDMC)]; JY, B lymphoblastoid line (a gift from Jack Strominger, Harvard University); HeLa, cervical carcinoma and the murine fibroblast line, 3T3 were utilized in these studies. Cells were obtained from the American Type Tissue Collection except as indicated.

Primary cells

B- and T-lymphocytes and monocyte/macrophages were independently isolated from freshly obtained normal human spleen using a Rosette-Sep Cell purification kit (Stem Cell Technologies). Discarded splenic tissue was obtained in accordance with the policies of the Institutional Review Board at BIDMC. The resultant cell preparations were examined by flow cytometry to confirm the purity of the individual cell populations using phycoerythrin (PE)-labeled mAbs to human IgG, CD19, CD3, CD14 and CD16 (Sigma-Aldrich). Purified dendritic cells were a generous gift from Dr David Avigan, BIDMC, and FDCs were a generous gift from Dr Arnold Freedman.

Yeast two-hybrid screen

A HeLa cDNA library, pGAD10-HeLa cDNA Matchmaker (Clontech), was screened with the pGBT.C-CD21.CT target plasmid. Briefly, plasmid DNA prepared from a single library amplification and pGBT.C-CD21.CT were co-transformed into the yeast strain, Y190 (Clontech) by the lithium acetate method. Approximately 10^6 independent clones were screened. Transformants were selected on the basis of their ability to activate both the GAL1::HIS3 and GAL1::lacZ reporter genes using standard procedures for yeast manipulations (Chien et al., 1991).

Yeast plasmid DNA was isolated and sequenced. To confirm the specificity of the candidate interactions, isolated plasmids were independently re-transformed into Y190 with either pGBT.C-CD21.CT or three unrelated target plasmids, encoding lamin (Bartel et al., 1996), bacteriophage T7 gene 2 (Bartel et al., 1996), or the intracellular domain of the Coxsackie and adenovirus receptor, CAR (Bergelson et al., 1997). Candidates that activated both reporter genes (as above) when co-transformed with pGBT.C-CD21.CT were considered true positives.

Cloning of full length HeLA FHOS cDNA

The full-length FHOS HeLa cDNA sequence was amplified from a Marathon-Ready™ human HeLa cDNA library (Clontech) using the FHOS-specific forward and reverse primers (5′ TGAGCCGGCC-GCAGAGCC 3′ and 5′ CGGGATCCTCACACCTCCAGGCCAG-GACC 3′) respectively. The Hela cDNA clone obtained was sequenced on both strands and deposited in GenBank under accession no. AY192154.

Demonstration of FHOS-CD21 interaction

In vitro

Initially GST-FHOS.CT, GST-EBV.TK (thymidine kinase) and GST alone were expressed and purified from BL21 carrying pGEX4T1-FHOS.CT, pGEX6P2-EBV.TK (Gustafson et al., 1998) and pGEX4T-1 vectors, respectively, using a glutathione-Sepharose 4B column (Amersham), and assessed for purity. Cell lysates were prepared from both Raji (CD21+) and Nalm6 (CD21-) cell lines. 10^7 cells were lysed in 0.5 ml of 1% NP-40 buffer supplemented with 1 mM of each of the following protease inhibitors: leupeptin, pepstatin, PMSF and aprotinin. The lysates were centrifuged at 800 ***g*** at 4°C for 10 minutes to remove cell debris and then incubated with 3 μg of purified (a) GST-FHOS.CT, (b) GST, or (c) GST-EBV.TK, overnight (o/n) at 4°C. For co-purification 0.1 ml of pre-washed glutathione-Sepharose 4B beads was added to each sample (a-c) and further incubated o/n at 4°C. Beads were then washed three times in 0.1% NP-40/1×TPBS (0.1% NP-40 in PBS and 0.05% Tween 20) and then once in PBS containing 0.5 M LiCl to remove non-specific proteins binding to the glutathione beads. The beads were boiled in sample buffer, separated by 7% SDS-PAGE and transferred to nitrocellulose (Osmonics) by electroblot. The nitrocellulose filter was pre-blocked in 1×TPBS 5% powdered milk (Carnation) o/n, incubated with rabbit anti-CD21 serum (Prota et al., 2002) (diluted 1:250 in 1×TPBS/5% milk) for 2 hours at room temperature (RT), washed in 1×TPBS, incubated with goat anti-rabbit-HRP secondary Ab (1:3000 dilution in 1×TPBS/5% milk) for 20 minutes at RT, re-washed and developed with chemiluminescent substrate, ECL (Amersham).

In vivo

An EGFP-modified version of the mammalian MATCHMAKER two-hybrid assay (Clontech, Catalog no. K1602-1) was used to confirm in vivo FHOS-CD21 interaction. To increase the sensitivity of the reporter activity the chloramphenicol acetyl transferase (CAT) reporter gene in pG5CAT was replaced with EGFP (Clontech). Briefly, the CAT open reading frame was removed from pG5CAT by PCR with Pfu polymerase (Stratagene) using the forward and reverse primers, 5′ GA*AGATCT*TTTAGCTTCCTTAGCTCC 3′ (*BglII*) and 5′ ATAAGAAT*GCGGCCGC*TTGCCCTTAAACGCCTGGTGC 3′ (*NotI*), respectively. The PCR product (pG5ΔCAT) was ligated with the EGFP gene isolated from pEGFPN2 by *Bgl*II and *Not*I digestion. The resulting plasmid was named pG5ΔCAT-EGFP.

To generate bait and target vectors containing either FHOS.CT or CD21.CT both genes were amplified, introducing unique (*Eco*RI) restriction sites for subcloning. The primers used were as follows: 5′ CG*GAATTC*CAGGCGGCCCGTGAAGTGCGCATCATGC 3′ and 5′ CG*GAATTC*TCACACCTCCAGGCCAGGACC 3′ (for FHOS.CT) and 5′ CG*GAATTC*AAACACAGAGAACGC 3′ and 5′ CG-*GAATTC*TCAGCTGGCTGGGTTGTATGG 3′ (for CD21.CT). To generate bait vectors, FHOS.CT (966-1164) and CD21.CT (1000-1033) were fused with the GAL4 DNA binding domain generating the clones pM-FHOS.CT and pM-CD21.CT, respectively. To generate target vectors FHOS.CT (966-1164) and CD21.CT (1000-1033) were fused to the VP16 activation domain, generating the clones pVP16-FHOS.CT and pVP16-CD21.CT, respectively. 293T cells were co-transfected using Lipofectamine 2000™ (Invitrogen) with 0.5 μg of pG5ΔCAT-EGFP plus each of the following combination of plasmids: (1) pM3-VP16 (+ control) (2) pM-53 + pVP16-T (+ control) (3) pM-53 + pVP16-CP (– control) (3) pM-FHOS.CT + pVP16-CD21.CT and (4) pM-CD21.CT + pVP16-FHOS.CT. Additionally, the bait and target vectors were co-transfected with an irrelevant corresponding positive control vector (pM-53 or pVP16-T). Twenty-four hours later cells were fixed and analyzed by fluorescence microscopy.

Fluorescence microscopy

For indirect immunofluorescence cells were plated into 12-well trays at 2×10^5 cells/well. Co-localization studies were performed with cells (293T, HeLa) that were transfected with 1 μg of pEGFP-FHOS, pEGFP-FHOSΔCT, or pBABE-CD21 alone or in combination as stated. At selected time points after transfection cells were fixed and stained as outlined below and imaged using the Eclipse E600 fluorescence microscope (Nikon) at either 40× or 100× magnification employing Spot Advance for image capture and processing (Diagnostic Instruments). Twenty-four hours after transfection cell nuclei were stained with Hoechst 33342 (Molecular Probes) and fixed with 4% paraformaldehyde in 0.1 M phosphate buffer (PB) (0.2 M $NaH_2PO_4.H_2O$, 0.2 M $NaHPO_4$, pH 7.2) for 30 minutes at RT. Fixed cells were permeabilized with 0.1% Triton X-100/PB/3% BSA for 15 minutes at RT and extensively washed with PB. For actin staining, fixed cells were incubated with TRITC-labeled phalloidin (Sigma-Aldrich) in 1% BSA/PB (1:20,000 dilution) for 1 hours at RT. For α-tubulin staining fixed cells were incubated with anti-α-tubulin mAb (clone B-5-5-1-2, Sigma-Aldrich) in 1% BSA/PB at a 1:200 dilution for 1 hour at RT, washed and then visualized by staining with goat $F(ab')_2$ anti-mouse IgG R-PE (Biosource) in 1% BSA/BP at 1:200 dilution for 1 hour at RT. All cells were mounted using AquaPoly/mount (Polysciences). For CD21 staining, fixed cells (above) were incubated with anti-CD21 mAb HB-5 (Tedder et al.,

1984) in 1% BSA/PB (10 μg/ml) for 1 hour at RT and visualized as described for tubulin.

For ligand challenge experiments, prior to fixation, cells were incubated with either concentrated EBV, prepared and purified as described previously (Prota et al., 2002), concentrated Kaposi's sarcoma-associated herpesvirus (Dezube et al., 2002) or with polyclonal rabbit anti-CD21 SCR1-SCR2 antisera (Prota et al., 2002) diluted 1:100 in PB. This antiserum does not block binding of mAb HB-5, which recognizes SCR4 of CD21 (Carel et al., 1990). Pre-immune serum was used as a control. Cells were washed three times in PB, fixed and developed for CD21 localization as above; UPC10 (IgG2a) was the isotype matched control for HB-5.

RT-PCR

Total RNA was prepared from cells using a RNeasy Mini kit (Qiagen). RT-PCR was performed using a GeneAmp kit (Roche) with 1 μg of total RNA prepared from relevant cells, using FHOS (MG112 and MG113) and GAPDH-specific primers (MG121 5′ GCCATGAG-GTCCACCACCCTGT 3′ and MG122 5′ CTACTGGCGCTGCCA-AGGCTGT 3′).

In situ hybridization

Non-radioactive in situ hybridization was performed as described previously (Berger and Hediger, 2001) using a digoxigenin-labeled cRNA probe containing 3496 nucleotides (ATG – STOP codon) of FHOS cDNA, which had been first cloned into the pGEMT vector (Promega) to facilitate preparation of an antisense probe. Control sections were incubated in an identical concentration of the sense FHOS probe.

Results

The cytoplasmic domain of CD21 interacts with the C-terminus of FHOS

To identify candidate proteins that interact with the cytoplasmic domain of human CD21 a modified version of Field's yeast two-hybrid assay (Fields and Song, 1989) was utilized (see Materials and Methods). A vector, CD21.CT (target) expressing the cytoplasmic 34 aa of human CD21 was synthesized and then co-transformed into yeast with a HeLa cDNA vector library (bait). A positively identified transformant was sequenced and shown to contain an 858 bp insert predicting an open reading frame of 199 aa (966-1164) followed by a stop codon and 3′ untranslated sequence. The complete DNA sequence encoding a 1164 aa protein was subsequently cloned and found to be identical to FHOS (Westendorf et al., 1999). The HeLa cDNA fragment identified encodes the carboxyl terminus 199 aa of FHOS. This is a variable region located C-terminal to the highly conserved formin homology domains (FH1/FH2) that may confer unique interaction(s) to different formin family members (Evangelista et al., 2003; Wallar and Alberts, 2003).

Following identification of the HeLa FHOS fragment, the full length HeLa cDNA clone was amplified by PCR (GenBank accession no. AY192154) using a HeLa cDNA library as a template. Comparison of splenic and HeLa derived-sequences revealed 13 nucleotide alterations that resulted in 9 predominantly conservative aa changes (E264D, E359D, S387T, D633E, V634L, T700S, R689Q, E745G, G751E, D849E) all located upstream of the C-terminal CD21 interactive domain. As expected, HeLa-derived FHOS contained the predicted domains that are conserved among diverse formin family members (Wallar and Alberts, 2003; Westendorf, 2001; Westendorf et al., 1999;) including the FH domains, two coil-coiled domains, a collagen-like domain and a putative diaphanous autoregulatory domain (DAD)-like domain (Wallar and Alberts, 2003). The latter is proposed to link the N terminus with the C terminus in an intramolecular inhibitory interaction.

To verify the specificity of the CD21-FHOS interaction a direct yeast two-hybrid assay was performed. The bait vector containing the C terminus of FHOS was co-transformed with CD21.CT (the original target vector) or with CD21-TMCT, a related vector which contains nine amino acids from the adjacent transmembrane of CD21, together with three control target vectors expressing unrelated proteins. As shown in Fig. 1a, activation of the HIS3 (and LacZ, data not shown) reporter gene only occurred in co-transformants that expressed CD21.CT (or CD21-TMCT) together with the C terminus of FHOS (Fig. 1a). These findings confirm that FHOS-CD21 interaction is specific and highly reproducible in yeast.

CD21 expressed in human cells interacts with FHOS

To determine whether FHOS could interact with endogenous CD21 that is expressed on the plasma membrane of human B-lymphocytes a bacterial vector linking GST with the C-terminal 199 aa residues of FHOS was generated to enable expression and purification of a GST-FHOS fusion protein. GST-FHOS was then immobilized on glutathione-Sepharose and used to precipitate CD21 from freshly prepared cell membrane lysates originating from B-cell lines. After elution, GST-FHOS and its bound ligand(s) were analyzed by immunoblot using both an anti-GST Ab to confirm the elution of the GST-FHOS fusion protein and using an anti-CD21 Ab to confirm the presence of CD21 as a FHOS-interacting protein on the column. When cell lysates prepared from CD21+ Raji cells were used (Fig. 1b, lane 4), CD21 could be readily detected in the fraction eluted from GST-FHOS. No protein was detected when lysates from the CD21-Nalm6 line was identically analyzed (Fig. 1b, lane 6). When GST-FHOS was replaced with GST alone or with GST-TK (irrelevant control) as the immobilized ligand, neither of the control ligands bound CD21 (Fig. 1b, lanes 2 and 3). As shown in Fig. 1b**,** lane 1, the size of CD21 detected in Raji cell lysates was the same as that of CD21 co-precipitated by FHOS. These results demonstrate that FHOS interacts with endogenously expressed CD21 from cell membrane lysates of human B-cells confirming that the FHOS-CD21 interaction first identified in yeast occurs in vitro.

FHOS interacts with CD21 in vivo

To demonstrate the in vivo interaction between FHOS and CD21 a modified version of the mammalian two-hybrid system (Clontech) was employed in which the reporter vector enzyme CAT was replaced with the fluorescent protein EGFP and cells were analyzed by fluorescence microscopy to visualize EGFP (see Materials and Methods). First the fluorescent two-hybrid assay was validated using the bait (pM) and target (pVP16) control vectors provided by the manufacturer (positive control: pM3-VP16 and pM-53+pVP16-T and negative control: pM-53+pVP16-CP) as shown in Fig. 1c, top. Both bait and target vectors were then generated that contained either FHOS.CT (C

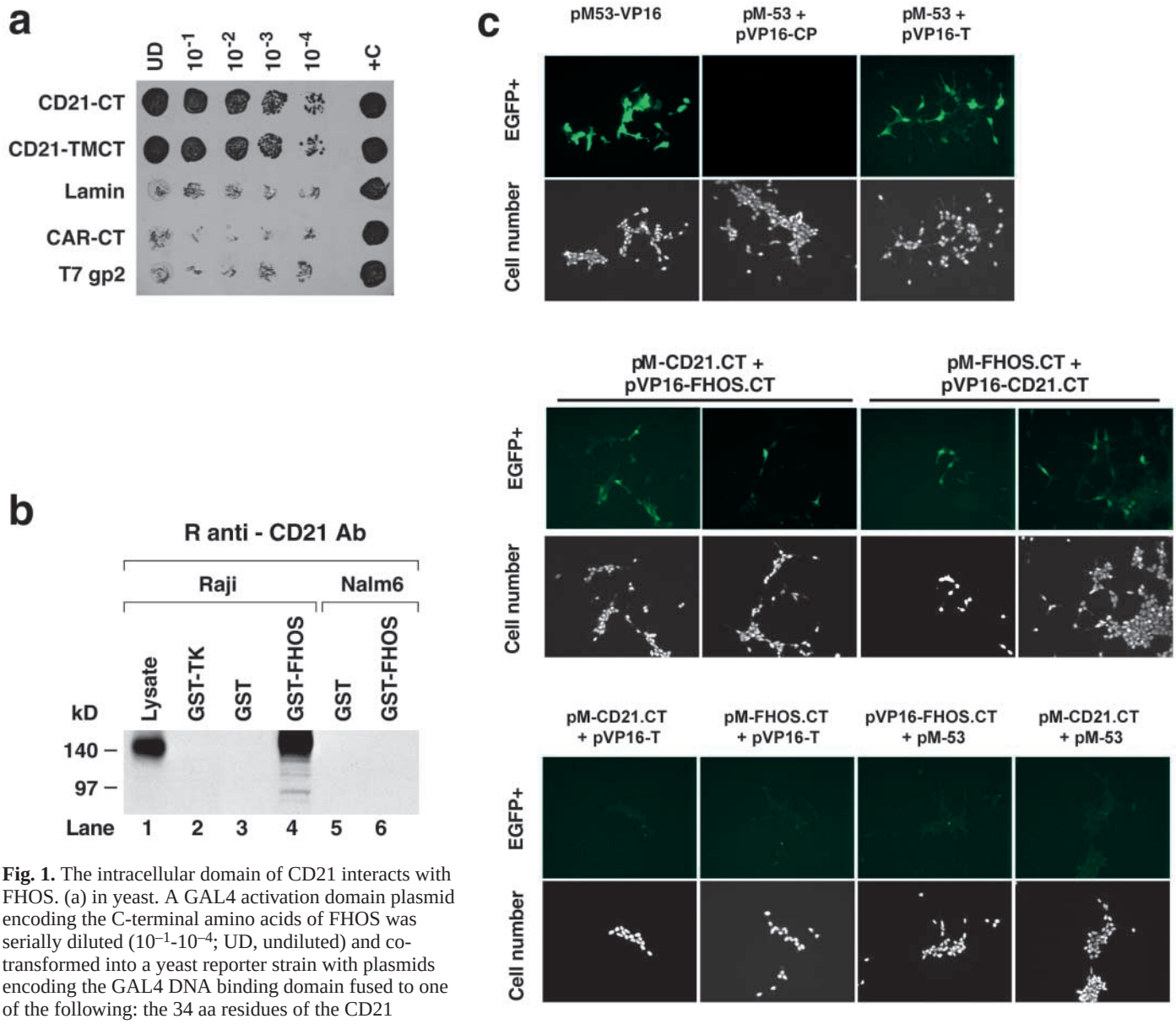

Fig. 1. The intracellular domain of CD21 interacts with FHOS. (a) in yeast. A GAL4 activation domain plasmid encoding the C-terminal amino acids of FHOS was serially diluted (10^{-1}-10^{-4}; UD, undiluted) and co-transformed into a yeast reporter strain with plasmids encoding the GAL4 DNA binding domain fused to one of the following: the 34 aa residues of the CD21 cytoplasmic tail (CD21-CT), the 34 aa residues of the CD21 cytoplasmic domain plus nine residues of the transmembrane domain (CD21-TMCT), lamin, the 105 aa residues of the CAR cytoplasmic domain (CAR-CT), or bacteriophage T7 gene 2 (T7/gp2; see Materials and Methods). Co-transformants were selected on minimal medium. Growth (i.e. activation of the HIS3 reporter) indicates a positive interaction. +C (positive control) represents co-transformation of plasmids encoding SNF1 and SNF4, proteins that interact in the two-hybrid assay. (b) In vitro. Purified fusion proteins expressing the C terminus of FHOS, GST-FHOS, GST alone or GST-TK (irrelevant protein) were incubated with cell lysates prepared from the B-cell lines Raji (CD21+; lanes 2-4) and Nalm6 (CD21–; lanes 5 and 6). Proteins interacting with FHOS were co-purified on glutathione beads, separated by SDS-PAGE and detected by immunoblot using a monospecific rabbit anti-CD21 antiserum. A total protein lysate from Raji cells (lane 1) was analyzed as a CD21 positive control. (c) In vivo. 293T cells were transfected with pG5ΔCAT-EGFP (reporter) plus the desired combination of bait (pM-X) and target (pVP16-X) vectors as indicated. X denotes the fusion protein of interest. Twenty-four hours after transfection, cells were identified with Hoechst (nuclear stain), fixed, and analyzed by fluorescence microscopy. Fluorescent EGFP+ cells indicates a positive interaction between bait and target fusion proteins. Top panel (method verification): EGFP induction was assessed using positive control vectors (pM53-VP16 and pM-53 + pVP16-T) compared with negative control vectors (pM-53 + pVP16-CP, control protein; Clontech). Middle panel: EGFP induction following co-transfection of recombinant vectors encoding the cytoplasmic domain of CD21, CD21.CT together with the C terminus of FHOS, FHOS.CT. Right and left panels show reciprocal experiments. Bottom panel (control), EGFP induction following transfection of CD21.CT or of FHOS.CT together with cognate two-hybrid vectors encoding irrelevant proteins (T antigen or p53).

terminus, 966-1164) or CD21.CT (cytoplasmic domain, 1000-1033), i.e. pM-FHOS.CT, pM-CD21.CT, pVP16-FHOS.CT and pVP16-CD21.CT to enable confirmation of protein interaction in reciprocal assays. First, the recombinant vectors were individually transfected into 293T cells together with the modified reporter vector, pG5ΔCAT-EGFP, to ensure that no auto-activation of the reporter EGFP gene occurred (not shown). Next both combinations of the bait and the target

vector (i.e. pM-FHOS.CT/pVP16-CD21.CT and pM-CD21.CT/pVP16-FHOS.CT) were co-transfected into 293T cells along with pG5ΔCAT-EGFP. As seen in Fig. 1c middle, each combination of the bait and target proteins was able to interact in 293T cells inducing expression of the fluorescent reporter. For additional controls both the bait and target vectors were transfected with a corresponding control plasmid provided by the manufacturer (e.g. pM-CD21.CT + pVP16-T) (Fig. 1c, bottom) to ensure absence of nonspecific EGFP induction. These results demonstrate that in mammalian cells, the C terminus of FHOS is able to specifically interact with the cytoplasmic domain of human CD21.

FHOS distribution and co-localization with actin

Next, a series of experiments were undertaken to analyze the cell biology of the FHOS-CD21 interaction. First a eukaryotic expression vector encoding full length FHOS fused at the N-terminus to the enhanced green fluorescent protein (EGFP), generating pEGFP-FHOS, was utilized to assess the cellular distribution of FHOS in live cells. pEGFP-FHOS was transfected into 293T cells and 24 hours later the cells were imaged by fluorescence microscopy. As shown in Fig. 2a, panels 1 and 2, FHOS localized to the cytoplasm of the cell, where it was observed surrounding the nuclear membrane, though it was excluded from the nucleus itself as demonstrated by Hoechst staining (Fig. 2a, panels 5 and 8). FHOS accumulated at the cell periphery (Fig. 2a) and at the borders between two cells (Fig. 2b). However, FHOS was most apparent close to the leading edge where it was prominently observed in filopodia, microspikes (Fig. 2a, panel 2) and in small lamellipodia (Fig. 2a, panels 3 and 6). Fig. 2a, panel 6 further demonstrates FHOS accumulation along one side of the nucleus as well as at the tips of elongating protrusions. These findings are consistent with the integral role of formins in the regulation of actin organization (Pelham and Chang, 2002; Tolliday et al., 2002). Coordinate staining to detect both actin (TRITC-phalloidin) (Fig. 2a, panel 4) and microtubules (α-tubulin, anti-mouse PE) (Fig. 2a, panel 7) further showed that FHOS specifically co-localizes with actin at the cell periphery and at the borders between cells (Fig. 2a panel 5 and Fig. 2b, panels 1-7), but does not co-localize with tubulin (Fig. 2a, panel 8). Remarkably, as shown in Fig. 2a, panel 3, overexpressed FHOS formed actin cables (inset), as has been reported for yeast formins (Feierbach and Chang, 2001; Sagot et al., 2002a). In the perinuclear region, the association of FHOS with actin was less prominent than at other locations (Fig. 2b, panels 1-3), as has been previously noted (Koka et al., 2003).

Aggregation and co-localization of CD21 and FHOS is dynamically enhanced in the presence of a cross-linking ligand

Based on the known functions of both CD21 and FHOS we hypothesized that the interaction of both proteins would be influenced by environmental and/or intracellular cues that occur only in vivo. To investigate the mechanics of this interaction in cells that lack CD19, 293T cells were initially co-transfected with both pEGFP-FHOS and pBABE-CD21 (a eukaryotic expression vector that encodes full length human CD21) in order to highly express the respective proteins (Fig. 3a). Twenty-four hours later the cells were analyzed with either a mAb directed to human CD21 (anti-CD21, HB-5) (Fig. 3a, panel 5) or with an isotype-matched control mAb, UPC10 (Fig. 3a, panel 2) or with second Ab alone, the latter to document

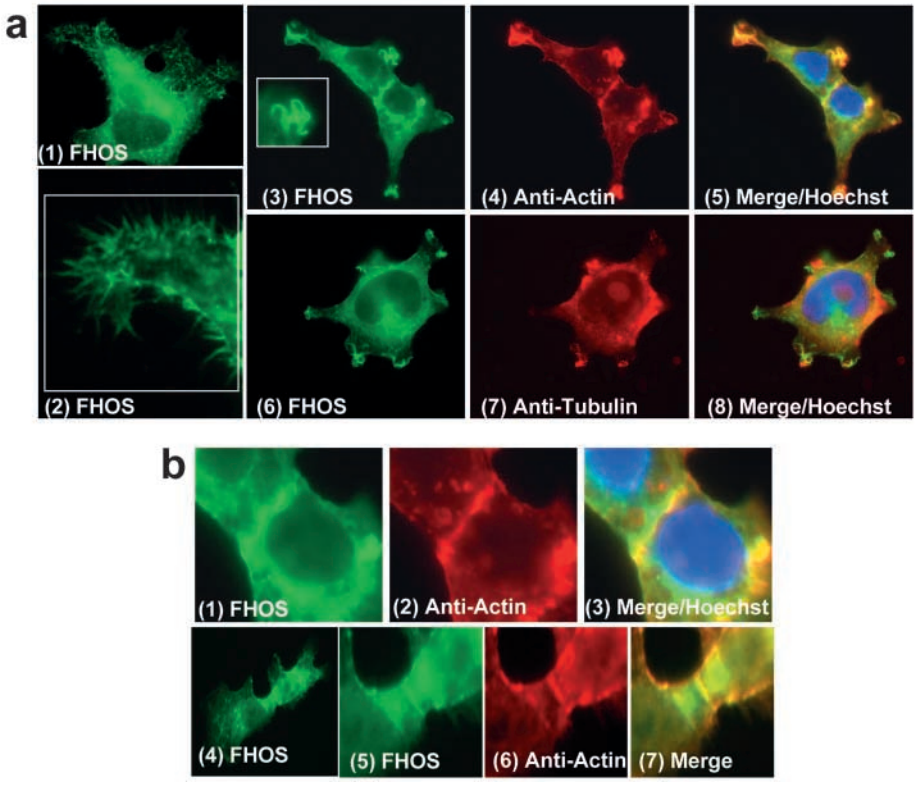

Fig. 2. FHOS associates with the actin cytoskeletion. (a) FHOS co-localizes with actin in the cytoplasm and in protrusions. Transfected 293T cells expressing full length FHOS fused to EGFP, FHOS (green, panels 1-3, 6) were co-stained with either TRITC-phalloidin (panel 4; red) to detect actin or with anti α-tubulin/goat $F(ab')_2$ anti-mouse Ig R-PE (panel 7; red). Merged images (panel 3 with 4 and panel 6 with 7) are shown in panels 5 and 8, respectively. Hoechst 33342 (blue) was used to detect nuclei in panels 5 and 8. (b) FHOS accumulates with actin at the border between cells and without actin in a perinuclear patch. Transfected 293T cells expressing EGFP-FHOS (green; panels 1,4-5) were co-stained with TRITC-phalloidin (panels 2 and 6; red) and merged images (panel 1 with 2 and panel 5 with 6) are shown in panels 3 and 7, respectively. Nuclei are stained blue as in a. All cells were fixed, stained and imaged using an Eclipse E600 fluorescence microscope and processed using Spot Advance technology.

the absence of non-specific FcR interactions (not shown). Examination of the cells by fluorescence microscopy revealed that CD21 was localized to the outer membrane of the cell (Fig. 3a, panel 5), whereas FHOS was predominately located in the cytoplasm, with some protein localized to patches under the outer plasma membrane (Fig. 3a, panels 1 and 4). Overlapping images for both overexpressed CD21 (red) and FHOS (green) demonstrated minimal co-localization (yellow) of both proteins, as shown in Fig. 3a, panel 6.

To address whether extracellular ligand engagement of CD21 alters its cellular localization relative to FHOS, epithelial cells expressing both CD21 and EGFP-FHOS were incubated with either purified EBV (or purified Kaposi's sarcoma-associated herpesvirus as a control) or with rabbit anti-CD21 Ab (or a pre-immune serum control). Attachment of Ab or EBV to CD21 is known to cause receptor cross-linking (dimerization in the case of antibody (IgG), multimerization in the case of virus), potentially leading to receptor redistribution within the plasma membrane.

When 293T cells were challenged with EBV, CD21 was redistributed into larger membrane patches and in some cells a more discrete cap-like structure could be observed (Fig. 3a, panel 8). Remarkably, in the regions where CD21 formed tight aggregates in the presence of EBV, some of the expressed FHOS protein coordinately re-localized with CD21 and accumulated in the same cap-like structures (Fig. 3a, panel 7). Merging of both images for CD21 (red) and FHOS (green) demonstrated the co-localization (yellow) of both proteins, especially in the cap-like structure, as shown in Fig. 3a, panel 9. Enhanced co-localization of both CD21 and FHOS was also observed when cells were challenged with rabbit anti-CD21 Ab, though it was less pronounced (not shown). The addition of either Kaposi's sarcoma herpesvirus or pre-immune serum did not cause redistribution of CD21 with FHOS in 293T cells.

To extend the observations obtained when using 293T cells, both EGFP-FHOS and EGFP-FHOSΔCT (FHOS 1-965, lacking the C-terminal 199aa/the CD21 interacting domain) were co-expressed with CD21 in a HeLa cell line. HeLa cells lack all HLA-Class II expression (Zhou et al., 1997) whereas 293T cells can express minimal HLA-DP (Fingeroth et al., 1999) (personal observation). Selection of the HeLa cell line for further study was based upon knowledge that HLA-Class II can act as a co-receptor for a distinct glycoprotein present on EBV, following initial attachment of EBV gp350 to CD21 (Li et al., 1997). The cellular distribution of FHOS, FHOSΔCT and CD21 were examined in HeLa cells, first in the absence (Fig.

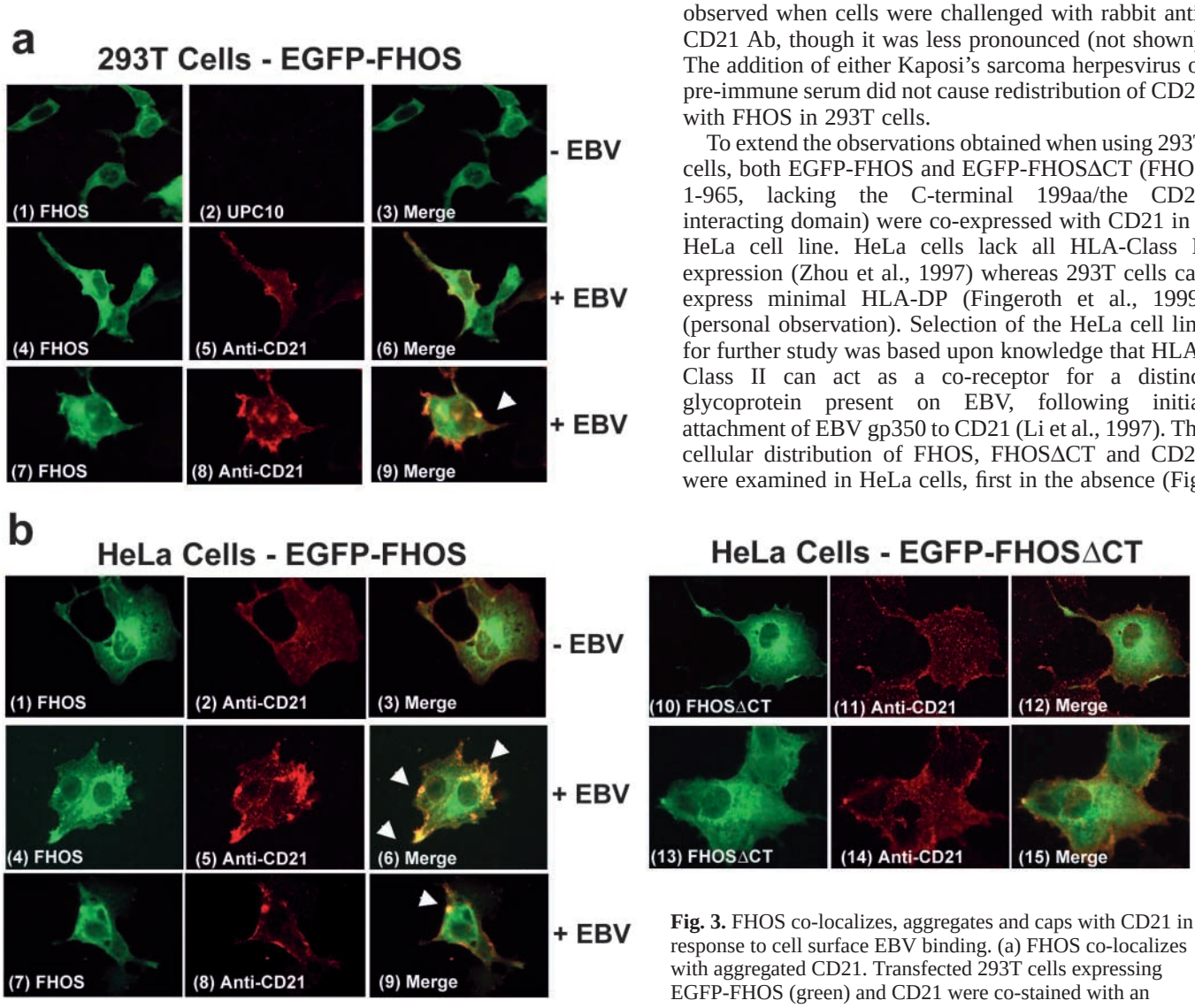

Fig. 3. FHOS co-localizes, aggregates and caps with CD21 in response to cell surface EBV binding. (a) FHOS co-localizes with aggregated CD21. Transfected 293T cells expressing EGFP-FHOS (green) and CD21 were co-stained with an isotype control mAb (UPC10; panel 2) or with anti-CD21 (mAb HB-5; panels 5 and 8) followed by goat $F(ab')_2$ anti-mouse IgG-R-PE (red). Cells challenged with concentrated EBV are shown in panels 4-9. Merged imaged (panel 4 with 5 and panel 7 with 8) are shown in panels 6 and 9 respectively. (b) The C terminus of FHOS is required for efficient aggregation and co-localization. Transfected HeLa cells expressing either FHOS (EGFP-FHOS, green; panels 1-9) or FHOSΔCT (EGFP-FHOSΔCT, green; panels 10-15) and CD21 (red; stained as in a) were incubated with EBV (panels 4-9 and 13-15) or without EBV (panels 1-3 and 10-12). Merged images of FHOS with CD21 are shown in panels 3 (panel 1+2), 6 (panel 4+5) and 9 (panel 7+8). Merged images for FHOSΔCT with CD21 are shown in panels 12 (panel 10+11) and 15 (panel 13+14). All cells were fixed, stained and imaged as stated in Fig. 2.

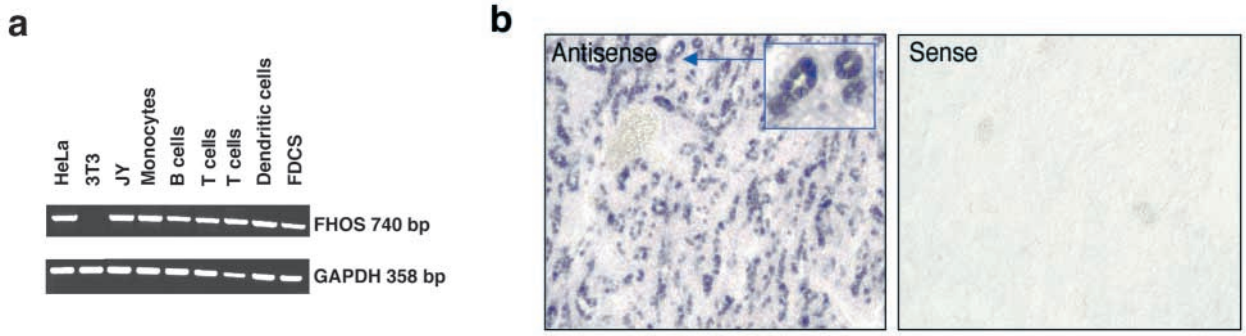

Fig. 4. FHOS is abundantly expressed in splenic littoral cells. (a) FHOS expression in primary hematopoietic cells. RT-PCR of total RNA was performed using internal FHOS-specific primers (Materials and Methods) and demonstrates the ubiquitous expression of FHOS RNA in distinct primary hematopoietic cells (B cells, T cells, monocytes, dendritic cells, FDCs) and certain cell lines (HeLa, JY). Negative control, murine 3T3 cells. (b) FHOS expression in spleen. Normal frozen human spleen was sectioned and analyzed by in situ hybridization. The antisense panel demonstrates high expression of FHOS mRNA in splenic littoral cells, whereas no signal can be detected in the sense panel (control).

3b, panels 1-3 and 10-12) and then in the presence (Fig. 3b, panels 4-9 and 13-15) of EBV.

In the absence of EBV, there was limited co-localization of FHOS and CD21 in HeLa cells (Fig. 3b, panels 1-3), identical to that observed in 293T cells. In the presence of EBV, CD21 re-localized and could be observed in concentrated aggregates as shown in Fig. 3b, panel 5, and even seen in dense cap-like structures (Fig. 3b panel 8). As expected, a portion of FHOS coordinately re-localized with CD21 into concentrated aggregates and cap-like structures as shown in Fig. 3b, panels 4 and 7 (compared to Fig. 3b, panels 5 and 8). Merging of the CD21 (red) and FHOS (green) images demonstrated that both FHOS and CD21 had specifically reorganized and aggregated, and accumulated at the same regions in the cell in response to EBV (Fig. 3b, panels 6 and also 9). Notably, in the absence of its CD21 interacting domain, FHOSΔCT failed to significantly co-localize with CD21 even in the presence of EBV (Fig. 3b, panels 13-15). FHOSΔCT did not appear to re-localize FHOS or cause significant stress fiber formation (Fig. 3b, panels 10 and 12 compared with 1 and 3).

FHOS RNA is highly expressed in skeletal muscle, hematopoietic tissue, lung and heart, but is completely absent from brain

Examination of an adult human tissue blot revealed an ~4 kb message, as previously reported (Westendorf et al., 1999), that was present in spleen, heart, lung, skeletal muscle, kidney, but not in brain (Fig. S1a, http://jcs.biologists.org/supplemental). Expression of FHOS mRNA in other tissues was analyzed by a Multiple Tissue Expression Array (MTE). The rank order of FHOS expression in these tissues was as follows: hematopoietic tissues including spleen, lymph nodes, bone marrow, peripheral blood lymphocytes, fetal liver > adult liver and, to a lesser extent, fetal and adult muscle, lung and heart > kidney and colon. However, FHOS mRNA was not detected in either whole adult or fetal brain tissue (Fig. S1b, http://jcs.biologists.org/supplemental). Furthermore, hybridization analysis of a MTE Array (Clontech) that contained spinal cord tissue as well as neural tissue obtained from 20 anatomic subdivisions of the brain failed to detect full length FHOS mRNA (not shown). These findings establish that although FHOS is expressed in many tissues, including tissues that do and do not express CD21, FHOS expression is not ubiquitous and is absent in the central nervous system. Of note, a related, but distinct human formin cDNA that maps to chromosome 18 (FHOS maps to 16), in GenBank as KIAA1695: hypothetical protein FLJ22297 (accession no. BAB21786) was obtained from brain.

FHOS is highly expressed in splenic littoral cells

Based on the observation that FHOS interacts with the cytoplasmic domain of CD21, we hypothesized that splenic ‘overexpression’ of FHOS as described by Westendorf (Westendorf et al., 1999) would localize to B-lymphocytes and FDCs where CD21 is expressed. To identify the splenic cell type that abundantly expresses FHOS we purified cell populations from the hematopoietic constituents of splenic white pulp (B-cells, T-cells, macrophages, dendritic cells and FDCs), using both splenic and peripheral blood sources of the respective lineages to prepare total RNA. Surprisingly, when analyzed semi-quantitatively by RT-PCR (Fig. 4a), the expression of FHOS mRNA in each cell population appeared approximately equivalent suggesting that abundant expression of FHOS RNA in spleen might result from cumulative expression of the transcript in white pulp. To test this hypothesis RNA in situ hybridization was performed on human splenic tissue using full-length FHOS cDNA as a probe. Surprisingly FHOS mRNA was most highly transcribed in the red pulp, specifically in a population of sinus lining cells known as littoral cells (Fig. 4b). Littoral cells express cell surface markers indicative of a mixed endothelial and histiocytic lineage, although they also express the T-cell marker CD8 (Buckley, 1991). Characterization of this ubiquitous red pulp cell type (~30% of cellular constituents) has in fact been quite limited (Arber et al., 1997; Hirasawa and Tokuhiro, 1970). To confirm that the FHOS-expressing cells were littoral cells, an adjacent section was fixed in formalin and analyzed by immunoperoxidase staining. This revealed expression of relevant antigens including von Willebrands factor and CD8 on morphologically identical cells (not shown). These studies demonstrate that FHOS is highly expressed in a specialized cell type that lines the vascular channels of the red pulp of human

and is believed to be important for antigen internalization and clearance.

Discussion

Formins are a family of actin binding proteins that are conserved throughout eukaryotic evolution (Wasserman, 1998; Zeller et al., 1999). They function in dynamic remodeling of the cytoskeleton thereby regulating cell polarity and migration, cytokinesis, trafficking of vesicles, signaling to the nucleus and cell survival (Tanaka, 2000; Wallar and Alberts, 2003; Wasserman, 1998; Zeller et al., 1999). In higher eukaryotes, these functions form the basis for control of embryonic development and organ formation. Nine mammalian formins have thus far been identified (Li and Higgs, 2003). In vivo, mutation of the C terminus of certain of these proteins has been associated with limb deformity (mouse formin1), renal aplasia (mouse formin1), deafness (human diaphanous1) and ovarian failure (human diaphanous2, mouse formin2) (reviewed by Leader et al., 2002).

Until recently formins were believed to function solely as molecular scaffolds providing a platform for crosstalk between signal transduction effectors (Rho family GTPases, src family kinases, wnt pathway proteins, others), actin binding proteins (profilin and profilactin binding proteins) and mediators of transcriptional regulation (activators of the serum-response transcription factor). Several critical studies now show that the highly conserved FH2 domain from yeast formins (Kovar et al., 2003; Pring et al., 2003; Pruyne et al., 2002; Sagot et al., 2002b) and from a mammalian formin, mDia1 (Li and Higgs, 2003) can directly nucleate the barbed ends of actin filaments leading to actin cable formation. This process is independent of assembly of branched actin filaments mediated by Arp2/3 complex and provides evidence for a separate cellular pathway of actin nucleation and dynamic control of cytoskeletal reorganization.

We show that FHOS, a human formin recently implicated in the regulation of cell motility (Koka et al., 2003) and vesicle trafficking [i.e. of IRAP/GLUT4 (insulin-responsive aminopeptidase/glucose transporter isoform type 4) bearing vesicles] (Tojo et al., 2003) binds to the short cytoplasmic domain of human CD21. The FHOS-CD21 interaction, which was originally identified using a yeast two-hybrid assay, was confirmed in vitro using a stringent GST-FHOS pull down assay to precipitate B-lymphocyte CD21 and was further verified in vivo using an EGFP-modified version of a mammalian two-hybrid assay. Interaction with CD21 occurs via the C-terminal amino acid residues of FHOS (aa 966-1164) in a region that encompasses a DAD-like domain and has been proposed to bind its own N terminus in an intramolecular inhibitory interaction (Westendorf, 2001). In the case of diaphanous-related formins this interaction is released upon binding of phosphorylated Rho GTPases to an N-terminal GTPase binding domain. Recently this region of FHOS has also been reported to interact with IRAP (Tojo et al., 2003). The significance of this overlapping FHOS domain is unknown, however, interestingly a related sequence in the short interactive region of each protein partner, ESSxK (in IRAP) and DTSxK (in CD21) can be identified (though this motif is not conserved in mCD21/mCD35). These findings suggest that human FHOS may participate in vesicle trafficking or more speculatively may regulate exo- and endocytosis. We are currently using our modified EGFP-mammalian two-hybrid technology to fine map the region(s) in both FHOS and CD21 that enables their specific interaction in vivo.

In addition to the direct binding experiments, the functional consequences of FHOS-CD21 interaction was directly visualized by overexpression of the full-length proteins in two epithelial lines. These cells lack CD19 (and also CD35; personal observation), a protein that complexes with the extracytoplasmic domains of CD21 on B-lymphocytes and is believed to mediate the B-cell effector functions linked to CD21 ligation and crosslinking (Fearon and Carroll, 2000; Poe et al., 2001). In the absence of a suitable antibody and to optimize visualization of intracellular distribution, EGFP fusion proteins were generated for both full length FHOS and FHOS lacking the C-terminal CD21 interactive domain. When expressed in cells both EGFP fusion proteins localized to the cytoplasm of the cell, as has been reported recently (Koka et al., 2003). EGFP-FHOS was present together with F-actin in leading edge structures where it could be clearly visualized in elongating lamellipodia as well as in filopodia, microspikes, regions of cell-cell contact, as well as at the contractile ring in dividing cells (not shown).

In cells that were co-transfected with both CD21 and FHOS, FHOS was predominately localized in the cytoplasm and CD21 was uniformly expressed along the cell surface, thus co-localization under these conditions was limited. However, when challenged with either EBV or polyclonal antibodies raised to the extracellular portion of CD21, both FHOS and CD21 coordinately re-localized forming aggregates and cap-like structures along the plasma membrane. When C-terminal truncated FHOS was utilized in these studies, even in the presence of EBV, neither re-localization of FHOS nor significant CD21 aggregation was observed. From the data obtained in this study we propose that upon extracellular ligand engagement of CD21 in vivo, FHOS binds to the cytoplasmic domain of CD21, in turn linking this membrane protein to the actin cytoskeleton. Formin attachment anchors the ligand bound receptor and provides physical control for CD21 re-localization in the form of aggregation and cap formation at the cell surface (Fig. 5).

The precise mechanisms that cause FHOS to redistribute to the cell membrane enabling it to interact with and co-aggregate CD21 are not known. FHOS recruitment may occur upon ligand induced modulation of intracellular CD21 (Barel et al., 2003) or may result from ligand-stimulated application of a mechanical force generating a physical and/or spatial cue (?GTPase activation, Rac1) that attracts FHOS proximate to CD21 (Riveline et al., 2001). Although the overall structural organization of FHOS is similar to that of diaphanous-related formins, important differences are suggested by the observation that Rac1 can bind FHOS in the absence of phosphorylation (and therefore activation). Furthermore, the location of the FHOS GTPase binding domain is altered relative to that of other formins and the results of transcription regulation studies suggest that Rac1 may function downstream rather than upstream of FHOS (Westendorf, 2001). Although FHOS contains a C-terminal DAD-like domain, the structure differs from that of diaphanous-related formins (Wallar and Alberts, 2003). Together with current findings (unpublished data) (Tojo et al., 2003) these observations raise the possibility

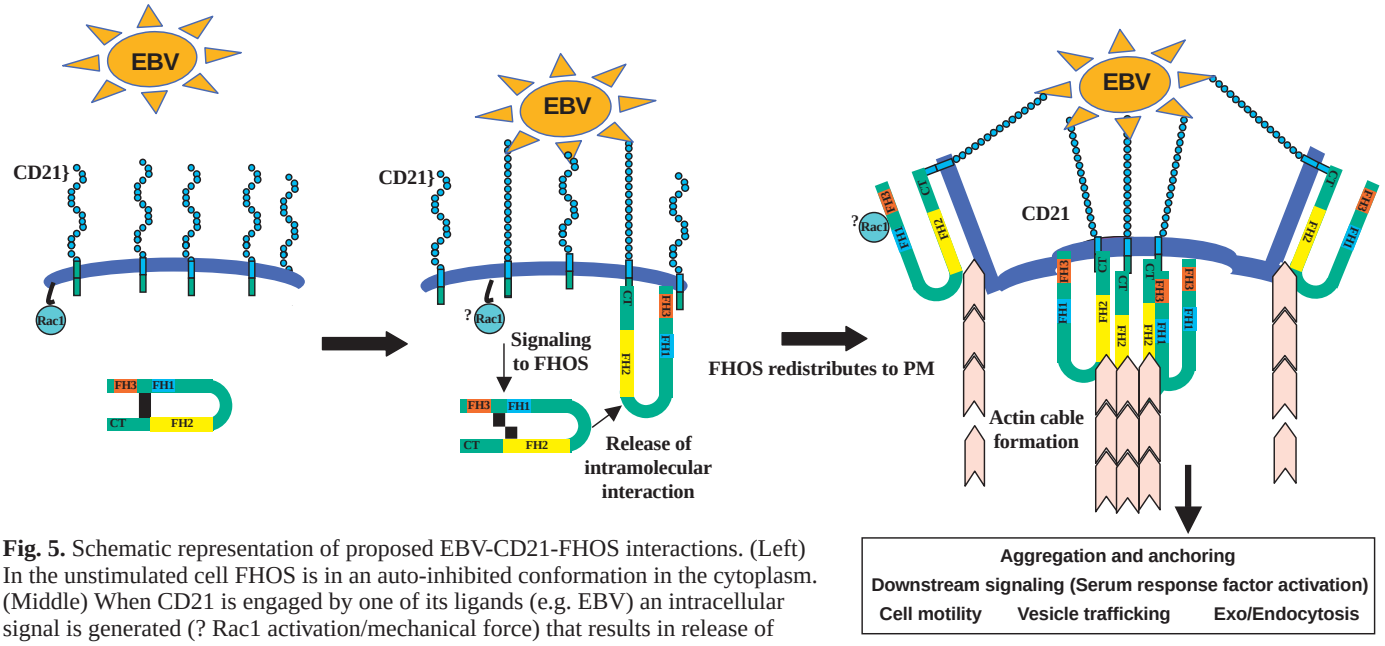

Fig. 5. Schematic representation of proposed EBV-CD21-FHOS interactions. (Left) In the unstimulated cell FHOS is in an auto-inhibited conformation in the cytoplasm. (Middle) When CD21 is engaged by one of its ligands (e.g. EBV) an intracellular signal is generated (? Rac1 activation/mechanical force) that results in release of nearby FHOS from intramolecular inhibition. FHOS unfolds and interacts with the cytoplasmic domain of CD21 via its unique C-terminal domain (CT). (Right) The exposed FH domains engage cytoskeleton associated-proteins and the FH2 domain nucleates actin leading to localized formation of actin cables. Actin clustering enables the physical relocalization of CD21 into membrane aggregates, provides an anchor for ligand bound CD21 and may regulate endocytosis.

that FHOS may initiate activation (release of intramolecular bonds and exposure of FH1/FH2) through interaction of the C-terminal DAD with specific membrane proteins, rather than through its N-terminal GTPase binding domain, which implies that FHOS is functionally distinct (Fig. 5, model). Irrespective of the mechanism of interaction, release of FHOS from a presumed autoinhibitory (intramolecular) conformation may further initiate or enhance actin polymerization through positive feedback loops (Wedlich-Soldner et al., 2003) and this could provide the first direct link to downstream signal transduction pathways initiated by CD21 alone (Fig. 5, model).

The discovery of two separate actin nucleation pathways suggests that cooperation between actin networks initiated by branched Arp2/3 complex nucleated filaments and by formin-mediated nucleation at barbed ends may represent a major mechanism for directing and enhancing actin assembly in mammalian cells (Svitkina et al., 2003). Recently in yeast, the conserved PCH family protein Cdc15, a protein critical for formation of the cytokinetic actin ring, was found to coordinate both nucleation pathways by binding directly to both the Arp2/3 complex activator Myo1p and the formin Cdc12p (Carnahan and Gould, 2003). In man, a Cdc15-like adaptor protein (CD2AP) interacts with the cytoplasmic domain of the T-cell co-receptor CD2 (Li et al., 1998), and this interaction has recently been linked via WASp interaction to Arp2/3 complex mediated nucleation. Although actin polymerization following CD2 ligation was impaired in a WAS/p (Arp2/3 complex activator)-deficient cell line (Badour et al., 2003), it was not abolished, suggesting other important interactions are involved. On the basis of several recent discoveries we speculate that physical ligation by immune complexes of both CD21 (formin) and immunoreceptor (Arp2/3 complex) actin nucleation pathways, particularly in lymphocytes that contain the GEF Vav (activator of Rac1) and WASp (activator of Arp2/3 complex), may alter the pattern and/or augment actin assembly at the immunoreceptor. These cytoskeletal alterations could contribute to aggregation of the BCR in microdomains, alter the rate of endocytosis or otherwise enhance signal transduction and lymphocyte activation. An understanding of precisely how ligand bound CD21 initiates actin assembly and of how this differs from patterns of actin cytoskeletal rearrangement initiated by ligation of the BCR or of CD19 may explain the unresolved mechanisms through which human CD21 functions: as a tether for C3d-bound antigen on FDCs, as a mediator of virus (and ligand) endocytosis on other cell types and as a lymphocyte co-receptor (for the BCR and other immunoreceptors).

Since FHOS was highly expressed in spleen we hypothesized that it would be abundant in either lymphocyte or FDC cell populations that also expressed CD21. Although FHOS was detected in many tissues and in most immortalized cell lines, in the majority of cases FHOS was more highly expressed in normal cells than in their cognate lines (data not shown). As FHOS RNA was not detected in human brain tissue or in cells of the central nervous system, FHOS is not a ubiquitously expressed protein. Unexpectedly, when we analyzed human spleen sections by RNA in situ hybridization, FHOS was most abundant in the splenic littoral cell. Littoral cells constitute more than 30% of the splenic red pulp (Hirasawa and Tokuhiro, 1970). They line the splenic sinusoids and display antigens consistent with a dual endothelial and histocytic lineage (Arber et al., 1997; Buckley, 1991). Littoral cells can extend long protrusions into the splenic sinuses and contain abundant intracellular vesicles. Therefore a role has been proposed for these cells in antigen capture, filtration and clearance – though no direct proof is available. Interestingly,

in the littoral cell angioma, a vascular tumor of red pulp that originates from littoral cells, the expression of CD21 is significantly upregulated (Arber et al., 1997).

Although implicated in organ malformation, thus far no abnormalities in splenic development have been linked to mammalian formins. FHOS maps proximate to the locus for the CREBBP gene on chromosome 16 and deletions of CREBBP are associated with Rubinstein-Taybi syndrome. Intriguingly, in a report about the association of some cases of Rubinstein-Taybi syndrome with polysplenia and hypoplastic heart it was suggested that a contiguous gene syndrome may sometimes occur (Bartsch et al., 1999).

In this study we identify FHOS as a novel CD21 interacting protein, a formin that binds the cytoplasmic domain of CD21 through its own carboxyl terminus, and itself re-localizes in the cell coordinately with CD21 at the plasma membrane upon specific ligand engagement of CD21. FHOS may provide CD21 with an independent and critical link to the cytoskeletal reorganization and interior signaling pathways of the cell.

This work was supported by an EIA from the American Heart Association and by National Institute of Health grants R01 DE12186 and K24 to J.D.F. We thank Rong Li, Evelyn Kurt-Jones and Cox Terhorst for helpful comments.

References

Arber, D. A., Strickler, J. G., Chen, Y. Y. and Weiss, L. M. (1997). Splenic vascular tumors: a histologic, immunophenotypic, and virologic study. *Am. J. Surg. Pathol.* **21**, 827-835.

Aubry, J. P., Pochon, S., Gauchat, J. F., Nueda-Marin, A., Holers, V. M., Graber, P., Siegfried, C. and Bonnefoy, J. Y. (1994). CD23 interacts with a new functional extracytoplasmic domain involving N-linked oligosaccharides on CD21. *J. Immunol.* **152**, 5806-5813.

Badour, K., Zhang, J., Shi, F., McGavin, M. K., Rampersad, V., Hardy, L. A., Field, D. and Siminovitch, K. A. (2003). The Wiskott-Aldrich syndrome protein acts downstream of CD2 and the CD2AP and PSTPIP1 adaptors to promote formation of the immunological synapse. *Immunity* **18**, 141-154.

Barel, M., Balbo, M., le Romancer, M. and Frade, R. (2003). Activation of Epstein-Barr virus/C3d receptor (gp140, CR2, CD21) on human cell surface triggers pp60src and Akt-GSK3 activities upstream and downstream to PI 3-kinase, respectively. *Eur. J. Immunol.* **33**, 2557-2566.

Bartel, P. L., Roecklein, J. A., SenGupta, D. and Fields, S. (1996). A protein linkage map of Escherichia coli bacteriophage T7. *Nat. Genet.* **12**, 72-77.

Bartsch, O., Wagner, A., Hinkel, G. K., Krebs, P., Stumm, M., Schmalenberger, B., Bohm, S., Balci, S. and Majewski, F. (1999). FISH studies in 45 patients with Rubinstein-Taybi syndrome: deletions associated with polysplenia, hypoplastic left heart and death in infancy. *Eur. J. Hum. Genet.* **7**, 748-756.

Bergelson, J. M., Cunningham, J. A., Droguett, G., Kurt-Jones, E. A., Krithivas, A., Hong, J. S., Horwitz, M. S., Crowell, R. L. and Finberg, R. W. (1997). Isolation of a common receptor for Coxsackie B viruses and adenoviruses 2 and 5. *Science* **275**, 1320-1323.

Berger, U. V. and Hediger, M. A. (2001). Differential distribution of the glutamate transporters GLT-1 and GLAST in tanycytes of the third ventricle. *J. Comp. Neurol.* **433**, 101-114.

Bonnefoy, J. Y., Henchoz, S., Hardie, D., Holder, M. J. and Gordon, J. (1993). A subset of anti-CD21 antibodies promote the rescue of germinal center B cells from apoptosis. *Eur. J. Immunol.* **23**, 969-972.

Bradbury, L. E., Kansas, G. S., Levy, S., Evans, R. L. and Tedder, T. F. (1992). The CD19/CD21 signal transducing complex of human B lymphocytes includes the target of antiproliferative antibody-1 and Leu-13 molecules. *J. Immunol.* **149**, 2841-2850.

Buckley, P. J. (1991). Phenotypic subpopulations of machrophages and dendritic cells in human spleen. *Scanning Microsc.* **5**, 147-157.

Carel, J. C., Myones, B. L., Frazier, B. and Holers, V. M. (1990). Structural requirements for C3d,g/Epstein-Barr virus receptor (CR2/CD21) ligand binding, internalization, and viral infection. *J. Biol. Chem.* **265**, 12293-12299.

Carnahan, R. H. and Gould, K. L. (2003). The PCH family protein, Cdc15p, recruits two F-actin nucleation pathways to coordinate cytokinetic actin ring formation in Schizosaccharomyces pombe. *J. Cell Biol.* **162**, 851-862.

Cherukuri, A., Cheng, P. C., Sohn, H. W. and Pierce, S. K. (2001). The CD19/CD21 complex functions to prolong B cell antigen receptor signaling from lipid rafts. *Immunity* **14**, 169-179.

Chien, C. T., Bartel, P. L., Sternglanz, R. and Fields, S. (1991). The two-hybrid system: a method to identify and clone genes for proteins that interact with a protein of interest. *Proc. Natl. Acad. Sci. USA* **88**, 9578-9582.

Copeland, J. W. and Treisman, R. (2002). The diaphanous-related formin mDia1 controls serum response factor activity through its effects on actin polymerization. *Mol. Biol. Cell* **13**, 4088-4099.

Dezube, B. J., Zambela, M., Sage, D. R., Wang, J. F. and Fingeroth, J. D. (2002). Characterization of Kaposi sarcoma-associated herpesvirus/human herpesvirus-8 infection of human vascular endothelial cells: early events. *Blood* **100**, 888-896.

Evangelista, M., Pruyne, D., Amberg, D. C., Boone, C. and Bretscher, A. (2002). Formins direct Arp2/3-independent actin filament assembly to polarize cell growth in yeast. *Nat. Cell Biol.* **4**, 260-269.

Evangelista, M., Zigmond, S. and Boone, C. (2003). Formins: signaling effectors for assembly and polarization of actin filaments. *J. Cell Sci.* **116**, 2603-2611.

Fearon, D. T. and Carroll, M. C. (2000). Regulation of B lymphocyte responses to foreign and self-antigens by the CD19/CD21 complex. *Annu. Rev. Immunol.* **18**, 393-422.

Feierbach, B. and Chang, F. (2001). Roles of the fission yeast formin for3p in cell polarity, actin cable formation and symmetric cell division. *Curr. Biol.* **11**, 1656-1665.

Fields, S. and Song, O. (1989). A novel genetic system to detect protein-protein interactions. *Nature* **340**, 245-246.

Fingeroth, J. D. (1990). Comparative structure and evolution of murine CR2. The homolog of the human C3d/EBV receptor (CD21). *J. Immunol.* **144**, 3458-3467.

Fingeroth, J. D., Weis, J. J., Tedder, T. F., Strominger, J. L., Biro, P. A. and Fearon, D. T. (1984). Epstein-Barr virus receptor of human B lymphocytes is the C3d receptor CR2. *Proc. Natl. Acad. Sci. USA* **81**, 4510-4514.

Fingeroth, J. D., Diamond, M. E., Sage, D. R., Hayman, J. and Yates, J. L. (1999). CD21-Dependent infection of an epithelial cell line, 293, by Epstein-Barr virus. *J. Virol.* **73**, 2115-2125.

Gustafson, E. A., Chillemi, A. C., Sage, D. R. and Fingeroth, J. D. (1998). The Epstein-Barr virus thymidine kinase does not phosphorylate ganciclovir or acyclovir and demonstrates a narrow substrate specificity compared to the herpes simplex virus type 1 thymidine kinase. *Antimicrob. Agents Chemother.* **42**, 2923-2931.

Hirasawa, Y. and Tokuhiro, H. (1970). Electron microscopic studies on the normal human spleen: especially on the red pulp and the reticulo-endothelial cells. *Blood* **35**, 201-212.

Holers, V. M. (2000). Phenotypes of complement knockouts. *Immunopharmacology* **49**, 125-131.

Iida, K., Nadler, L. and Nussenzweig, V. (1983). Identification of the membrane receptor for the complement fragment C3d by means of a monoclonal antibody. *J. Exp. Med.* **158**, 1021-1033.

Koka, S., Neudauer, C. L., Li, X., Lewis, R. E., McCarthy, J. B. and Westendorf, J. J. (2003). The formin-homology-domain-containing protein FHOD1 enhances cell migration. *J. Cell Sci.* **116**, 1745-1755.

Kovar, D. R., Kuhn, J. R., Tichy, A. L. and Pollard, T. D. (2003). The fission yeast cytokinesis formin Cdc12p is a barbed end actin filament capping protein gated by profilin. *J. Cell Biol.* **161**, 875-887.

Leader, B., Lim, H., Carabatsos, M. J., Harrington, A., Ecsedy, J., Pellman, D., Maas, R. and Leder, P. (2002). Formin-2, polyploidy, hypofertility and positioning of the meiotic spindle in mouse oocytes. *Nat. Cell Biol.* **4**, 921-928.

Lee, S. W., Bonnah, R. A., Higashi, D. L., Atkinson, J. P., Milgram, S. L. and So, M. (2002). CD46 is phosphorylated at tyrosine 354 upon infection of epithelial cells by Neisseria gonorrhoeae. *J. Cell Biol.* **156**, 951-957.

Li, F. and Higgs, H. N. (2003). The mouse formin mDia1 is a potent actin nucleation factor regulated by autoinhibition. *Curr. Biol.* **13**, 1335-1340.

Li, Q., Spriggs, M. K., Kovats, S., Turk, S. M., Comeau, M. R., Nepom, B. and Hutt-Fletcher, L. M. (1997). Epstein-Barr virus uses HLA class II as a cofactor for infection of B lymphocytes. *J. Virol.* **71**, 4657-4662.

Li, J., Nishizawa, K., An, W., Hussey, R. E., Lialios, F. E., Salgia, R.,

Sunder-Plassmann, R. and Reinherz, E. L. (1998). A cdc15-like adaptor protein (CD2BP1) interacts with the CD2 cytoplasmic domain and regulates CD2-triggered adhesion. *EMBO J.* **17**, 7320-7336.

Martin, D. R., Marlowe, R. L. and Ahearn, J. M. (1994). Determination of the role for CD21 during Epstein-Barr virus infection of B-lymphoblastoid cells. *J. Virol.* **68**, 4716-4726.

Melamed, I., Stein, L. and Roifman, C. M. (1994). Epstein-Barr virus induces actin polymerization in human B cells. *J. Immunol.* **153**, 1998-2003.

Moir, S., Malaspina, A., Li, Y., Chun, T. W., Lowe, T., Adelsberger, J., Baseler, M., Ehler, L. A., Liu, S., Davey, R. T., Jr et al. (2000). B cells of HIV-1-infected patients bind virions through CD21-complement interactions and transmit infectious virus to activated T cells. *J. Exp. Med.* **192**, 637-646.

Moore, M. D., Cooper, N. R., Tack, B. F. and Nemerow, G. R. (1987). Molecular cloning of the cDNA encoding the Epstein-Barr virus/C3d receptor (complement receptor type 2) of human B lymphocytes. *Proc. Natl. Acad. Sci. USA* **84**, 9194-9198.

Morgenstern, J. P. and Land, H. (1990). Advanced mammalian gene transfer: high titre retroviral vectors with multiple drug selection markers and a complementary helper-free packaging cell line. *Nucleic Acids Res.* **18**, 3587-3596.

Pelham, R. J. and Chang, F. (2002). Actin dynamics in the contractile ring during cytokinesis in fission yeast. *Nature* **419**, 82-86.

Poe, J. C., Hasegawa, M. and Tedder, T. F. (2001). CD19, CD21, and CD22: multifaceted response regulators of B lymphocyte signal transduction. *Int. Rev. Immunol.* **20**, 739-762.

Pring, M., Evangelista, M., Boone, C., Yang, C. and Zigmond, S. H. (2003). Mechanism of formin-induced nucleation of actin filaments. *Biochemistry* **42**, 486-496.

Prodinger, W. M. (1999). Complement receptor type two (CR2,CR21): a target for influencing the humoral immune response and antigen-trapping. *Immunol. Res.* **20**, 187-194.

Prota, A. E., Sage, D. R., Stehle, T. and Fingeroth, J. D. (2002). The crystal structure of human CD21: implications for Epstein-Barr virus and C3d binding. *Proc. Natl. Acad. Sci. USA* **99**, 10641-10646.

Pruyne, D., Evangelista, M., Yang, C., Bi, E., Zigmond, S., Bretscher, A. and Boone, C. (2002). Role of formins in actin assembly: nucleation and barbed-end association. *Science* **297**, 612-615.

Riveline, D., Zamir, E., Balaban, N. Q., Schwarz, U. S., Ishizaki, T., Narumiya, S., Kam, Z., Geiger, B. and Bershadsky, A. D. (2001). Focal contacts as mechanosensors: externally applied local mechanical force induces growth of focal contacts by an mDia1-dependent and ROCK-independent mechanism. *J. Cell Biol.* **153**, 1175-1186.

Sagot, I., Klee, S. K. and Pellman, D. (2002a). Yeast formins regulate cell polarity by controlling the assembly of actin cables. *Nat. Cell Biol.* **4**, 42-50.

Sagot, I., Rodal, A. A., Moseley, J., Goode, B. L. and Pellman, D. (2002b). An actin nucleation mechanism mediated by Bni1 and profilin. *Nat. Cell Biol.* **4**, 626-631.

Svitkina, T. M., Bulanova, E. A., Chaga, O. Y., Vignjevic, D. M., Kojima, S., Vasiliev, J. M. and Borisy, G. G. (2003). Mechanism of filopodia initiation by reorganization of a dendritic network. *J. Cell Biol.* **160**, 409-421.

Tanaka, K. (2000). Formin family proteins in cytoskeletal control. *Biochem. Biophys. Res. Commun.* **267**, 479-481.

Tanner, J., Weis, J., Fearon, D., Whang, Y. and Kieff, E. (1987). Epstein-Barr virus gp350/220 binding to the B lymphocyte C3d receptor mediates adsorption, capping, and endocytosis. *Cell* **50**, 203-213.

Tedder, T. F., Clement, L. T. and Cooper, M. D. (1984). Expression of C3d receptors during human B cell differentiation: immunofluorescence analysis with the HB-5 monoclonal antibody. *J. Immunol.* **133**, 678-683.

Tojo, H., Kaieda, I., Hattori, H., Katayama, N., Yoshimura, K., Kakimoto, S., Fujisawa, Y., Presman, E., Brooks, C. C. and Pilch, P. F. (2003). The formin family protein, formin homolog overexpressed in spleen, interacts with the insulin-responsive aminopeptidase and profilin IIa. *Mol. Endocrinol.* **17**, 1216-1229.

Tolliday, N., VerPlank, L. and Li, R. (2002). Rho1 directs formin-mediated actin ring assembly during budding yeast cytokinesis. *Curr. Biol.* **12**, 1864-1870.

Wallar, B. J. and Alberts, A. S. (2003). The formins: active scaffolds that remodel the cytoskeleton. *Trends Cell Biol.* **13**, 435-446.

Wasserman, S. (1998). FH proteins as cytoskeletal organizers. *Trends Cell Biol.* **8**, 111-115.

Wedlich-Soldner, R., Altschuler, S., Wu, L. and Li, R. (2003). Spontaneous cell polarization through actomyosin-based delivery of the Cdc42 GTPase. *Science* **299**, 1231-1235.

Westendorf, J. J. (2001). The formin/diaphanous-related protein, FHOS, interacts with Rac1 and activates transcription from the serum response element. *J. Biol. Chem.* **276**, 46453-46459.

Westendorf, J. J., Mernaugh, R. and Hiebert, S. W. (1999). Identification and characterization of a protein containing formin homology (FH1/FH2) domains. *Gene* **232**, 173-182.

Zaffran, Y., Destaing, O., Roux, A., Ory, S., Nheu, T., Jurdic, P., Rabourdin-Combe, C. and Astier, A. L. (2001). CD46/CD3 costimulation induces morphological changes of human T cells and activation of Vav, Rac, and extracellular signal-regulated kinase mitogen-activated protein kinase. *J. Immunol.* **167**, 6780-6785.

Zeller, R., Haramis, A. G., Zuniga, A., McGuigan, C., Dono, R., Davidson, G., Chabanis, S. and Gibson, T. (1999). Formin defines a large family of morphoregulatory genes and functions in establishment of the polarising region. *Cell Tissue Res.* **296**, 85-93.

Zhou, H., Su, H. S., Zhang, X., Douhan, J., III and Glimcher, L. H. (1997). CIITA-dependent and -independent class II MHC expression revealed by a dominant negative mutant. *J. Immunol.* **158**, 4741-4749.